Thrust Area 4: Solar (Advanced PV Device Program)

Beyond Photovoltaics - Nanoscale Rectenna for Conversion of Solar and Thermal Energy to Electricity

PI: ShekharBhansali, **Co-PIs:** Elias Stefanakos, Yogi Goswami, Subramanian Krishnan
Students: Rudran Ratnadurai, Electrical Engineering/ Ph.D., Michael Celestin, Chemical Engineering/ Ph.D. Justin Boone, Electrical Engineering/ Ph.D.

Description: The main objective of the proposal is to commercialize and scale up a new technology, rectenna to convert waste heat energy to electricity. Although the prediction of highly efficient (~85%) solar rectennas was published almost 30 years ago, serious technological challenges have prevented such devices from becoming a reality. Since the ultimate goal of a direct optical frequency rectenna photovoltaic power converter is still likely a decade away, we plan to convert optical solar radiation to thermal radiation (~30 THz regime) using an innovative blackbody source. Leveraging the research efforts of the world-class team members, we plan to further develop the rectenna technology that is within reach of efficient radiation conversion at 30 THz. A fully integrated, blackbody converter and 30 THz rectenna system will be capable of converting at least 50% of solar and thermal energy into usable electrical power, clearly demonstrating a truly transformational new technology in the renewable energy technology sector.

Budget: $$598,500
Universities: USF
External Collaborators: Bhabha Atomic Research Center, India, Florida International University, Miami

Progress Summary

Objectives:

The research objective of this project is to develop a high efficiency solar/ thermal energy conversion using antenna coupled MIM tunnel junction. Towards this, the follow tasks were charted,

- Fabrication, characterization and testing of Metal-Insulator-Metal tunnel junction,
- Design, fabrication and testing of antenna,
- Integration of antenna and MIM junction.

Approach:

- Determine the AC and DC behavior of SAM based MIM using a novel microinjection contact
- Characterize the organic insulator layer to yield reliable electrical response
- Investigate the effect of varying the oxygen concentration on tunneling response of MIM junction
- Determine the efficiency and gain of the antenna

Accomplishments:

- MIM junctions with nanometer thin SAM layer was successfully deposited on Au and made contact with liquid metal to determine the electrical behavior. The organic tunnel junctions exhibited highly asymmetric I-V response with 1:200 rectification ratio.
- Nickel oxide layer was deposited with varying oxygen gradient, which exhibited a novel electrical response when subjected to low frequency AC measurement. The Device exhibited clipping behavior, which could be reproduced reliably. Moreover, the devices were tested over a period of time and observed to be reliable.
- A novel antenna structure consisting of dual design was developed and was observed to resonant at the designed frequency with 25% bandwidth. The radiation pattern also matches with the simulated plot.

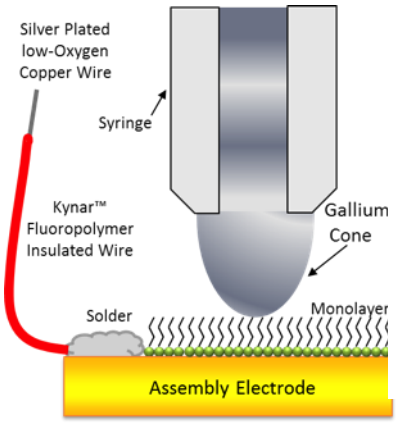

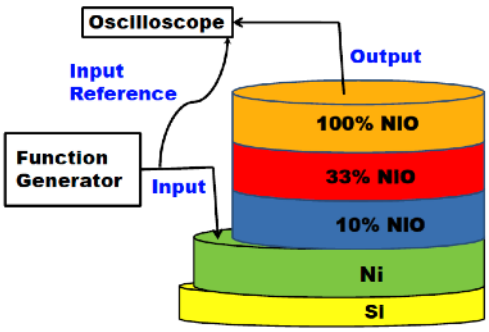

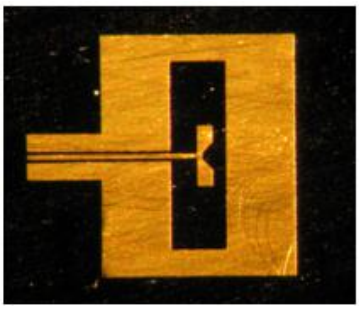

Funds leveraged/new partnerships created:
We have submitted a proposal to NSF in collaboration with UCF for an Engineering Research center. The proposal is entitled "*Nanosystems Engineering Research Center for Transformational Sensor and Detection Systems".*

We are currently collaborating with Bhabha Atomic Research Center, India in developing a organic based tunnel junction.

2011 Annual Report

Based on the research objective, during the current reporting period of the project, the main focus was to characterize the tunnel junction with organic insulator. As a preliminary approach, several organic films (self-assembled monolayers) were procured and characterized for the thickness uniformity using impedance spectroscopy technique. A novel-processing scheme was used, which incorporates microinjection of liquid metal to small contact areas. MIM tunnel junctions were fabricated with Au-SAM-Ga. In order to provide better electrical behavior, the SAM layer was optimized to yield maximum uniformity. Furthermore, the MIM junctions fabricated with inorganic insulator layer using NiO as the insulator layer was investigated for its electrical characteristics by varying the oxygen concentration in the NiO layer. Specifically, the gas ratio used for depositing the inorganic insulator layer was varied and its effect on electrical behavior of the junction was determined. Additionally, a folded dipole-slot antenna operating at 60 GHz were deigned, fabricated and characterized.

Research Accomplishments

1. Fabrication and Characterization of Self-assembled monolayer based MIM junction

Self-assembled monolayers (SAMs) have been explored for possible use as a dielectric in tunnel junctions for THz rectenna applications. Modeling of device performance was done in MATLAB with a custom modified BDR equation. Automated experimental trace to model fitting successfully deduces barrier heights and tunneling parameters from measured data.

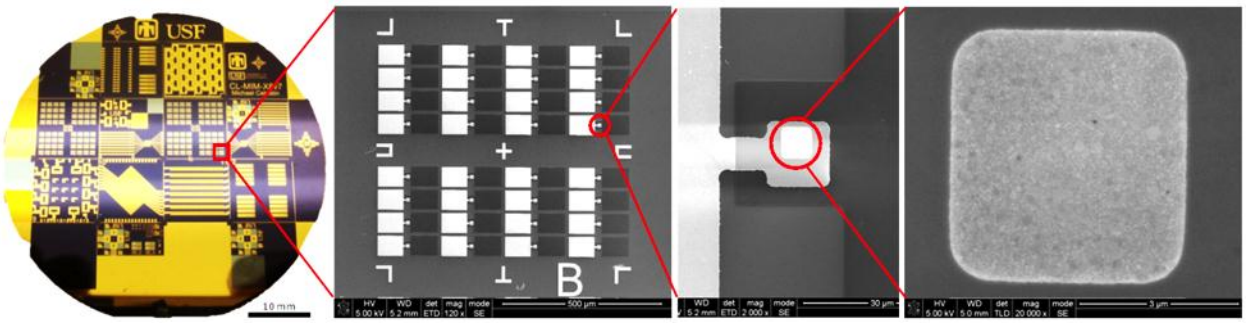

Figure 1: Two-inch (50mm) diameter wafer at left holding all test structures fabricated at the Center for Integrated Nanotechnology (CINT). Inset to the right (b) 32-element probe pad diode array, inset (c) detailed SEM of single diode junction, inset (d) process control detail of junction area.

A focus on fabrication of evaporation test structure resulted in a wafer scale integrated test structure. Fabrication was performed at the Center for Integrated Nanotechnology (CINT) in Albuquerque, NM. The device contains thousands of junctions of varying sizes and contact styles down to 0.5 µm features (Figure 1).

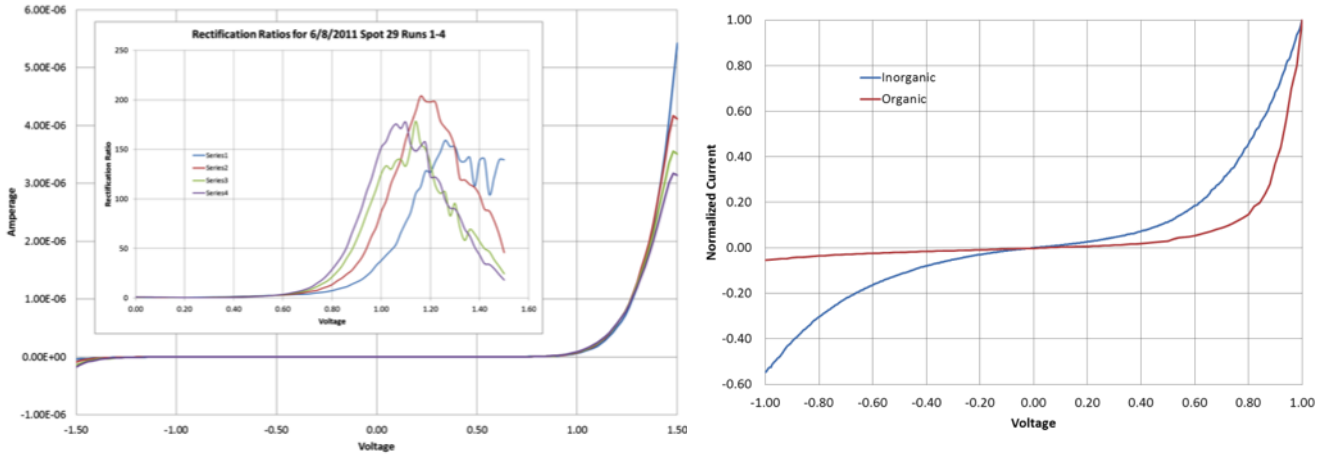

Figure 2: (a) I-V plot showing of hybrid SAM-Gallium Oxide tunnel junction. Inset, high rectification ratios for aforementioned IV traces reaching up to 200:1. (b) Comparison of Inorganic and Organic tunnel diode performance by normalized current response.

Selection of appropriate SAMs for optimum rectification performance was assisted by a liquid metal test setup employing a Gallium (or Mercury) filled syringe, goniometer stage, and Keithley 2400 source meter. Using this setup, DC performance was studied through a number of SAMs. High performance was seen using Gallium as a top metal and 1H,1H,2H,2H-Perfluorodecanethiol (Figure 2a). Comparing these results to similarly constructed Ni-NiOx-Cr, inorganic tunnel diodes, organic-based devices demonstrate superior performance (Figure 2b). Following these experiments, improvement of the test setup was done to improve noise and minimize complications in the AC domain yet to be tested (Figure 3). AC testing requires full modeling of parasitics to subtract for accurate test results; the modeling of these parasitics in addition to preliminary measurements has been completed.

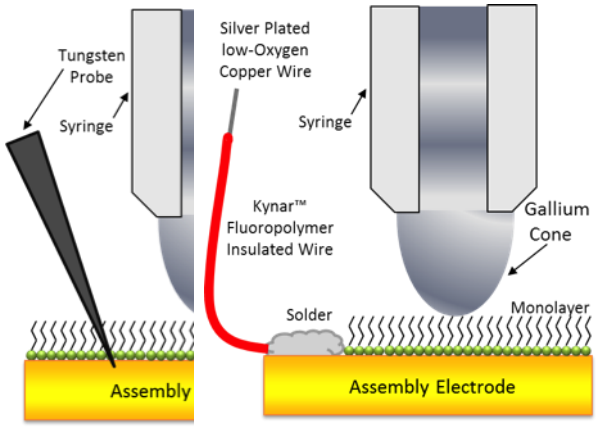

Figure 3: Graphic showing improvement of electrical connection with assembly electrode. Tungsten probe contact was a source of noise and inconsistency in measurement and remedied by directly soldering wire to the base.

2. Development of inorganic MIM junction using metal-oxide gradient film

Trilayer gradient NiO stack was done by sputtering Ni on 500nm thick SiO_2 on a Silicon substrate followed by sputter deposition of the NiO layers with oxygen concentrations of 10%, 33% and 100%. The percentage of the O_2 content in NiO was controlled by setting the O_2 to Ar flow ratios

such that the partial pressure of O_2 was 10% of the total gas pressure during sputtering for 10% NiO layer. The same procedure was followed when depositing NiO layers having 33% of O_2 (NiO (33%). The depositions of the first two layers of NiO were done at 30W. For the 100% NiO layer (NiO(100%), plasma was struck using only O_2 gas and was done at 50W since O_2 is lighter than Ar and more power is required for the momentum transfer process. The base pressure was 3 µTorr and the deposition pressure was 3mTorr while depositing Ni and 30mTorr while depositing the NiO layers. Pre-sputtering of the Ni target for 5 min was done while depositing both Ni layer and the NiO layers to avoid any contamination. After the deposition of each NiO layer, a wait period of about 10 min was given so as to allow an interface to form.

Figure 4 shows layout of device and measurement setup that we used to measure AC signal (1Hz to 5 MHz and peak voltage 100mV to 6V) propagation through the thin film stack ({Ni/NiO(10%)/NiO(33%)/NiO(100%)}(A)) where input signal was passing from function generator through Ni to the film and output signal was collected via tungsten tip to oscilloscope. It was observed that below 20 kHZ signal, output signal follows the input signal whereas beyond 20 kHz signal, peak of output signal starts getting clipped symmetrically as shown in figure 5 for 1MHz. For clear visibility of clipping, a plot of input voltage vs output voltage for all frequency mentioned above is shown in figure 6 where the clipping voltage (Vc) is marked. It was found that Vc changes with frequency for example at 50 KHz frequency and 1V signal; Vc is 0.8V, which decreases to 0.65V for 1MHz frequency. Peak voltage dependent clipping properties of the device was also investigated. It was found that at signal voltage below 200mV, the clipping characteristics were not observed for any frequency range. It was also observed that Vc increases along with the gradual increase of input peak voltage from 200mV to 5V for a particular frequency e.g. 1MHz. Above 5V peak voltage signal, clipping property of the stacks is lost (breakdown); and thereafter, output has same sine wave nature as input. Interestingly, after one and half hour of breakdown, film restarts showing clipping properties.

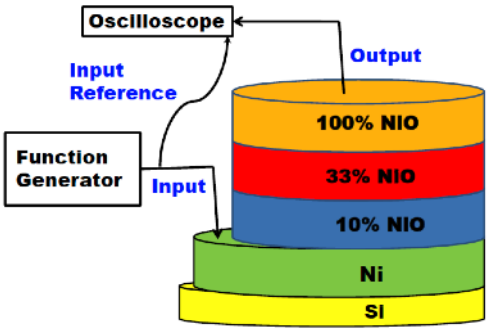

Figure 4: Schematic diagram of measurement setup and device structure for trilayer NiO stack

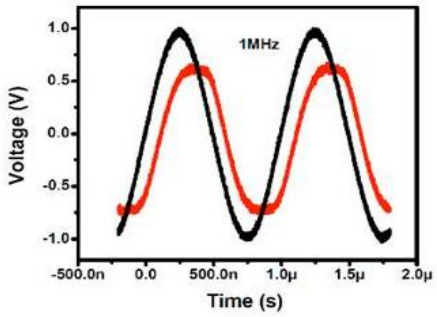

Figure 5: Typical input and ouput characteristics for 1V signal of frequency 1MHz

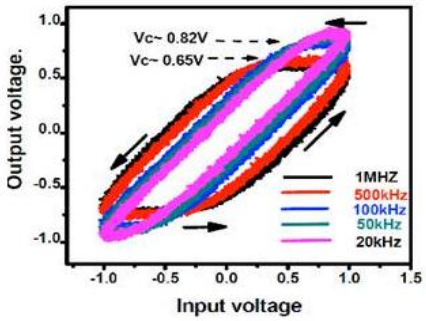

Figure 6: The input voltage vs output voltage. Arrows indicates direction of AC cycle.

To further study the effect of oxide gradient, a new stack [{Ni/NiO(10%)/NiO(50%)/NiO(100%)}(B)] was deposited where the middle layer was deposited at 50% oxygen [NiO(50%)] and the remaining two layers were deposited as the same as in stack A. The new stack B also shows clipping characteristics similar to that shown by stack A, except that Vc at1MHz and 1V signal changes to 0.6V. Clearly, change of oxide concentration gradient has an effect on Vc.

A new stack was designed where Ni interlayer was sandwiched between each oxide layer [device structure {Ni/NiO(10%)/Ni/NiO(33%) /Ni/NiO(100%)}C)]. The stack C also showed clipping properties under AC siganal. Clipping properties were observed for months under constant AC signal. All devices (A, B and C) were measured in ambient condition. This shows the robustness of the device properties. DC measurement of stacked films A, B and C revealed nonlinear, asymmetric, and non-hysteric current- voltage (*I-V*) characteristics as shown in figure 7. In DC measurement, Ni was bottom contact and tungsten tip as top contact. The analysis to understand clipping properties of NiO gradient stack is underway.

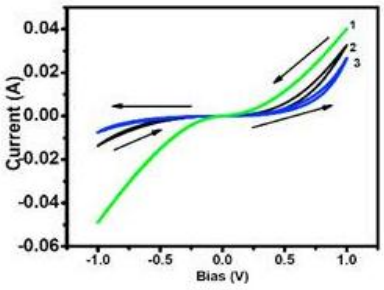

Figure 7: Current- voltage (I-V) characterization of samples A, B, C where voltage was cycled.

3. Modeling and characterization of a high frequency antenna

In this task, we present the design, fabrication and testing of a CPW-fed folded dipole slot antenna supported by a 50 µm silicon membrane, operating at 60 GHz. Silicon was chosen due to its easy integration abilities with traditional fabrication technologies. The folded dipole antenna included in the slot, provides wide bandwidth performances with multi-frequency band operations. This antenna structure is also scalable and can be integrated with current commercial devices. The layout of the folded dipole slot antenna is shown in Figure 8. The design and simulation of the antenna structure was performed using Agilent's Momentum Electromagnetic Simulator, which combines full-wave and quasi-static electromagnetic solvers for antenna modeling. A high resistive silicon substrate with infinite surface area was assumed for simulation purpose.

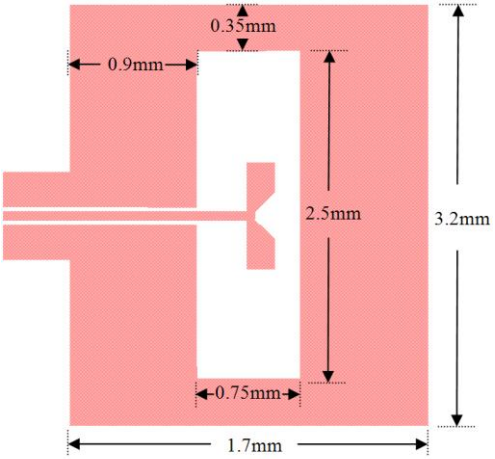

Figure 8: Momentum layout of 60 GHz slot antenna with folded dipole

The folded dipole slot antennas were realized on a 4" and 250 µm thick silicon substrate. Initially, silicon substrate was thermally oxidized to grow a 1 µm thick SiO_2 layer. Since the oxidation layer was required only on the membrane etch side, the oxide layer was chemically etched on the other side. While the oxidized side provided as an etch protectant layer during the micromachining process, the un-oxidized side served as the ground plane for the antenna. Following the oxide etch process, a photolithography step was performed to pattern the antenna and CPW configuration pads on the substrate. Then, a thin layer of chromium (Cr) and gold (Au) were deposited on the substrate. Cr was deposited with a thickness of ~ 30 nm and acted as an adhesion layer for the top Au (~300 nm) layer. After the contact pads were made, photolithography was performed on the backside of the substrate and windows were opened underneath the devices. The substrate was then subjected to a dry etching process, to micromachine the backside from 250 µm to 50 µm. Figure 9 (a) and (b) shows the microscopic image of the fabricated antenna and the membranes etched beneath the antenna in silicon, respectively.

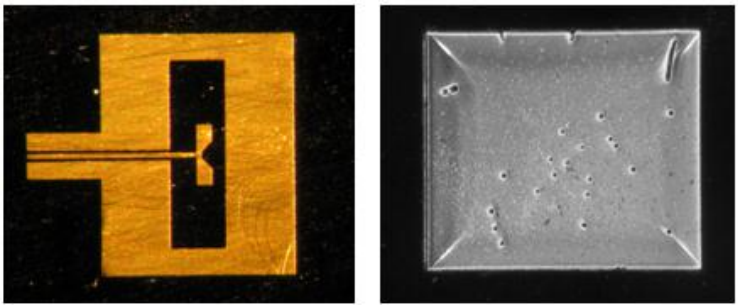

Figure 9: An Optical micrograph of fabricated 60 GHz folded dipole slot antenna on silicon

The simulated vs. measured reflection coefficient data of the antenna is illustrated in Figure 10. The figure shows that at 62 GHz, the antenna is well matched to 50Ω with a reflection coefficient of -45 dB. An additional resonance appeared at 55 GHz, which is contributed, to the antenna structure achieving multi-band operations. By minimizing the membrane thickness, additional surface waves were reduced and the antenna achieved a bandwidth of 25% at S11<-10 dB; improving the performance of previous silicon micromachined antennas. The antenna operates over a wideband from 50 to 65 GHz, proving its ability to be used in WLAN and V-band frequency applications. The discrepancy between data can be contributed to a variance in membrane thickness and losses caused by surface waves present during measuring.

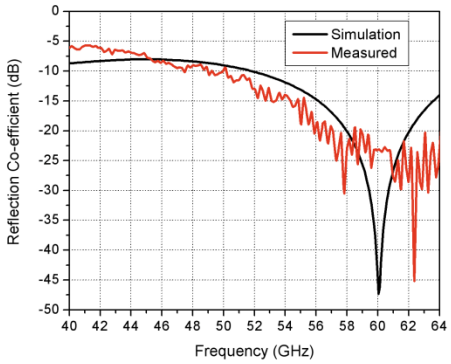

Figure 10: Measured vs. simulated reflection coefficient of the folded dipole slot antenna

Results obtained during the radiation pattern measurement are shown in Figure 11. The measured results are in good agreement with those achieved during simulation. The maximum co-polarization magnitude achieved was -8 dB at 0° with a gain of 4.1 dBi. This is the case because the pattern achieves maximum radiation at right angles to the dipole and drops off to zero on the antenna's axis. However, the slight difference in magnitudes of the measured vs. simulated patterns is due to inaccuracies during the measuring setup which requires precise positioning of the receiving antenna and stability in the angle guiding structure.

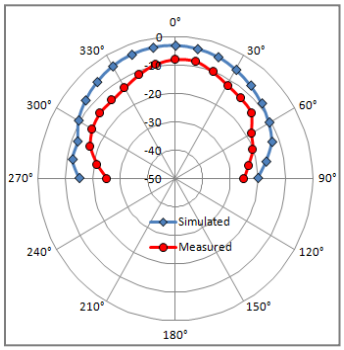

Figure 11: Measured vs. Simulated Co-Polarized E-plane radiation pattern (dB) of the 60 GHz antenna.

Journal and Conference publications:

1. R.Ratnadurai, S.Krishnan, E. Stefanakos, Y. Goswami, S. Bhansali, "Rectification properties of inorganic MIM Tunnel Junctions: A Review," Advanced Energy Materials, 2011. (Under Review)

2. S. Krishnan, J. Boone, S. Bhansali, "Membrane Supported 94 GHz Slot Antenna for Wideband Applications," IEEE Journal of Antennas and Propagation, 2011. (Under Review)

3. J. Boone, S. Krishnan, S. Bhansali, "CPW-fed Folded Dipole-Slot Antenna for WLAN Applications," IET Microwaves, Antenna and Propagation, 2011. (Under Review)
4. M. Celestin, S. Krishnan, E. Stefanakos, Y. Goswami, S. Bhansali, " Advances in SAM based MIM Tunnel Junctions," Chemical Review, 2011. (Under Review)

5. R.Ratnadurai, S. Koiry, S. Krishnan, S. Bhansali, E. Stfanakos, Y. Goswami, " NiO based thin film Clipper devices," FESC Summit, Gainesville, Sept 27-28, 2011.

6. M. Celestin, S. Krishnan, S, Bhansali, E. Stefanakos, Y. Goswami, " Current Trends in Micro and Nanotechnology based Energy Harvesting," NanoFL, Miami, Sept 30- Oct 1, 2011.

7. J. Boone, S. Krishnan, S. Bhansali, T. Weller, "Micromachined Vertical Coaxial Probes for Nanoscale Device Characterization," NanoFL, Miami, Sept 30- Oct 1, 2011.

8. S.P. Koiry, S. Krishnan, R. Ratnadurai, D.Y. Goswami, S. Bhansali, "Controlled ex-situ doping of electrochemically polymerized 5,10,15,20 tetrakis (4-hydroxyphenyl)-porphyrin (THPP) for hybrid switching circuits," ECS 220th meeting, Boston, Oct 9-14, 2011.

9. M. Celestin, S. Krishnan, D.Y. Goswami, E. Stefanakos, S. Bhansali, " Organic Tunnel Diodes Fabricated for Rectenna based IR Sensing Applications," Advances in Applied Physics and Materials Science Congress, Antalya, Turkey, May 12 -15, 2011.

10. M. Celestin, S. Krishnan, D.Y. Goswami, E. Stefanakos, S. Bhansali, " Fabrication and Modeling of Organic Tunnel Diodes," 3rd Annual USF Research Day, Tampa, FL, Oct 2010.

11. R. Ratnadurai, S.Krishnan, E. Stefanakos, D.Y. Goswami, S. Bhansali, "Design Analysis of MIM tunnel junctions," 3rd Annual USF Research Day, Tampa, FL, Oct 2010.

12. J. Boone, S.Krishnan, E. Stefanakos, D.Y. Goswami, S. Bhansali, "Design and Simulation of a Scalabe Dipole Fed Slot Antenna," 3rd Annual USF Research Day, Tampa, FL, Oct 2010.